Electrochemical impedance spectroscopy characterization of passive film formed on implant Ti–6Al–7Nb alloy in Hank's solution

I. C. LAVOS-VALERETO*, S. WOLYNEC
Department of Metallurgical and Materials Engineering, Polytechnic School of the University of São Paulo, Av. Prof. Mello Moraes, 2463 – CEP 05508-900 – São Paulo, SP, Brazil
E-mail: iclvaler@usp.br or lavosvaler@yahoo

I. RAMIRES, A. C. GUASTALDI
Department of Physical-Chemistry, Institute for Chemistry of São Paulo State University (UNESP), Araraquara, SP, Brazil

I. COSTA
Materials Science and Technology Centre, Institute for Energy and Nuclear Research (IPEN/CNEN), São Paulo, SP, Brazil

The influence of potential on electrochemical behavior of Ti–6Al–7Nb alloy under simulated physiological conditions was investigated by electrochemical impedance spectroscopy (EIS). The experimental results were compared with those obtained by potentiodynamic polarization curves. All measurements were carried out in Hank's aerated solution at 25 °C, at pH 7.8 and at different potentials (corrosion potential, 0 mV(SCE), 1000 mV(SCE), and 2000 mV(SCE)). The EIS spectra exhibited a two-step or a two-time constant system, suggesting the formation of a two-layer oxide film on the metal surface. The high corrosion resistance, displayed by this alloy in electrochemical polarization tests, is due to the dense inner layer, while its osseointegration ability can be ascribed to the presence of the outer porous layer.

Introduction

The titanium and its alloys are presently the most important materials for biomedical and dental implant applications. This is due to the formation on their surface of a passive film, consisting mainly of amorphous titanium dioxide, which is responsible both for their corrosion resistance and their biocompatibility [1, 2]. Moreover, this film favors also a very good osseointegration [3].

There has been already a significant effort to electrochemically characterize these materials in terms of their corrosion behavior. Pan *et al*. [4] investigated the electrochemical behavior of commercial pure titanium, performing corrosion potential vs. time and potentiodynamic polarization measurements, and electrochemical impedance spectroscopy (EIS) tests [1] in phosphate-buffered saline solution without and with H_2O_2 additions. González and Mirza-Rosca [2] performed EIS tests of titanium and several of its alloys (Ti–10Mo, Ti–10Al–10Mo, Ti–5Al–15Mo, Ti–5Al–4.5V and Ti–5Al–2.5Fe) in Ringer's solution. Silva *et al*. [5] carried out electrochemical characterization of oxide films formed on Ti–6Al–4V alloy implanted with Ir in phosphate-buffered saline solution.

In EIS tests, titanium and most of its alloys exhibit behavior typical of thin passive oxide film. The Nyquist plots display incomplete capacitive semicircles, and pure capacitive behavior (high corrosion resistance) has been observed for commercial pure Ti and for Ti–5Al–15Mo and Ti–7Al–4.5V alloys [2]. Most publications [1, 2, 5] reported Bode phase angle plots with only one time constant indicating a near-capacitive response by a phase angle close to $-90°$ and in the /Z/ Bode plots by a straight line with slope approaching -1 [2, 5]. On the other hand, results obtained by Venugopalan *et al*. [6] with Ti–6Al–4V alloy exhibited a two time constant system, which they related to a layered oxide consisting of a porous outer oxide and a barrier inner oxide.

Besides the above-cited alloys, the Ti–6Al–7Nb alloy has been recently enrolled in the list of metallic implant materials. This alloy is of the alpha–beta $(\alpha+\beta)$ structure type, with a microstructure comparable to that of the wrought Ti–6Al–4V alloy [7]. This alloy was developed because of the concern about the possible toxicity of vanadium ions released from the Ti–6Al–4V alloy [8]. According to Cai *et al*. [9] all these titanium alloys can potentially be used as casting alloys in prosthetic dentistry.

*Author to whom all correspondence should be addressed.

The corrosion resistance of the Ti–6Al–7Nb alloy has been compared with that of commercially pure titanium and various other titanium alloys (Ti–6Al–4V and Ti–13Nb–13Zr) in a study carried out by Cai *et al*. [9]. Their results showed that all the metals examined with the same surface condition had similar electrochemical behavior.

Nevertheless, the data on electrochemical behavior of this alloy are still scarce. The results of corrosion potential vs. time and potentiodynamic polarization measurements of this alloy were reported elsewhere [10].

The aim of present work was to obtain further information about the passive film formed on the Ti–6Al–7Nb alloy in Hank's solution, in order to better understand its ability both to protect the metal against corrosion and to osseointegrate. This information was searched with the EIS technique, which is able to provide reliable data for determination of the passive film structure.

Experimental

The Ti–6Al–7Nb alloy used in present investigation was acquired in form of a rod from IMI Titanium Limited, England. The working electrodes prepared from this rod consisted of flat discs 2.0 mm thick and 12 mm diameter. This alloy was submitted to a semi-quantitative chemical analysis by X-ray fluorescence technique and its results are given in Table I.

The surface preparation of these discs for electrochemical tests was as follows: the discs were first ground with 220 through 1200 grit SiC papers and then polished with diamond down to 6 μm and followed by 1 μm alumina-30% chrome oxide suspension, and finishing with 5% oxalyc acid solution. Later, each polished sample was rinsed with acetone and put in an ultrasonic cleaner for 10 min. Subsequently, it was rinsed with bi-distilled water and ethyl alcohol, and finally dried under a hot air stream.

The testing medium was a Hank's solution whose composition is given in Table II. This solution was prepared by Instituto Adolpho Lutz, São Paulo, SP, Brazil. All the tests were performed at 25 °C in naturally aerated solutions.

The potentiodynamic polarization curves were obtained in order to define the electrode potentials for the EIS measurements. They were determined in a three-electrode electrochemical cell containing 250 ml of electrolyte. A saturated calomel electrode (SCE) was used as the reference electrode and a graphite rod as the auxiliary electrode. The measurements were performed with a Princeton Applied Research potentiostat (Model 273 A). A microcomputer was employed for data acquisition. These measurements were carried out after 2 h immersion in Hank's solution, in the range from − 800 mV(SCE) to 2800 mV(SCE), at a scan rate of 1 mV s^{-1}. In order to obtain reliable results, the determination of potentiodynamic polarization curves was repeated three times. The corrosion potential (E_{corr}), corrosion current density (or corrosion rate) (i_{corr}) and polarization resistance (R_p) were determined from these curves using the 352 Soft Corr III program.

TABLE I Chemical composition of Ti–6Al–7Nb alloy determined by semi-quantitative X-ray fluorescent technique

Element	Ti	Al	Nb	Fe	Si	Ni	Cu
Weight %	86.85	5.70	7.10	0.25	0.08	0.01	0.01

TABLE II Chemical composition of Ti–6Al–7Nb alloy determined by semi-quantitative X-ray fluorescent technique

Component	Concentration (mol/L)
pH	7.8
NaCl	0.1369
KCl	0.0054
$MgSO_4.7H_2O$	0.0008
$CaCl_2 2H_2O$	0.0013
$Na_2HPO_4.2H_2O$	0.0003
KH_2PO_4	0.0004
$C_6H_{12}O_6H_2O$	0.0050
Red phenol 1%	0.0071

The EIS measurements were carried out using an Impedance/Gain-Phase Analyzer coupled to a Potentiostat–Galvanostat System (EG&G Parc, Model 273A), which was connected to a three-electrode electrochemical cell. All measurements were performed in Hank's solution at different potentials. The measurements at the corrosion potential were performed after 2 h immersion in the physiological solution at 25 °C. EIS results at the other potentials were obtained 30 min after the overpotential has been applied. The frequency ranged from 100 kHz to 5 mHz, and the amplitude used was set at 5 mV. Results were presented in terms of Nyquist and Bode plots. Data acquisition and analysis were performed with a microcomputer. The spectra were interpreted using the ZView program. Due to the distributed relaxation feature which was observed with the titanium oxide film on the Ti–6Al–7Nb alloy, a constant phase element (CPE) was used for data fitting instead of an ideal capacitor.

Results

A typical potentiodynamic polarization curve of Ti–6Al–7Nb alloy is shown in Fig. 1. A corrosion potential (E_{corr}) of − 424 mV(SCE) was measured. From this potential up to approximately 0 mV(SCE) the curve indicates a

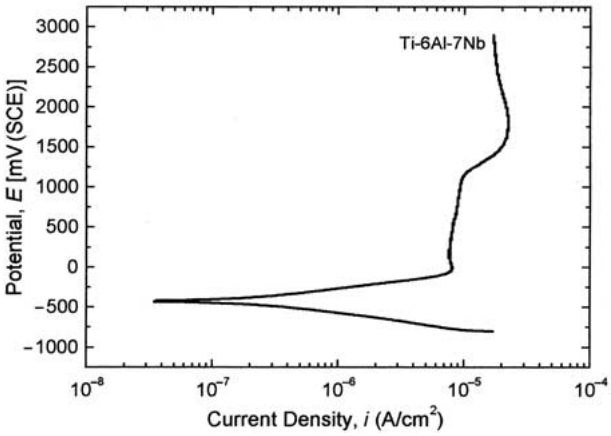

Figure 1 Potentiodynamic polarization curve of Ti–6Al–7Nb alloy in Hank's aerated solution at pH 7.8 and 25 °C. Scan rate: 1 mV/s.

TABLE III Average values of E_{corr}, i_{corr} and R_p determined for Ti–6Al–7Nb alloy from polarization curves obtained in Hank's aerated solution at pH 7.8 and 25 °C

E_{corr} [mV(SCE)]	i_{corr} ($\mu A/cm^2$)	R_p ($k\Omega./cm^2$)
-424 ± 10 (3)	-0.16 ± 0.14 (3)	225

*The number of tests is indicated in parentheses.

behavior typical of activation polarization, showing a well defined linear range, suggesting conformity to the Tafel's Law. The anodic Tafel slope (b_a) obtained at this region was nearly 128 mV. From 0 mV(SCE) up to 1200 mV(SCE) the curve shows a passive behavior, and a passive current density (i_{pp}) in the range of 0.8×10^{-5} to 1.0×10^{-5} A cm^{-2} was estimated. The current density increases at potentials around 1200 mV(SCE), and reaches a maximum (2.1×10^{-5} A cm^{-2}) at approximately 1800 mV(SCE), decreasing slightly afterwards. At the potential 2800 mV(SCE) a current density around 1.9×10^{-5} A cm^{-2} was measured. A detailed discussion of this polarization curve was presented elsewhere [10].

The average values of E_{corr}, i_{corr}, and R_p, from three different polarization curves determined by the 353 Soft Corr III program are presented in Table III.

The potentials for investigation of the electrochemical behavior of the Ti–6Al–7Nb alloy by EIS measurements were chosen from the above polarization curve. It was decided to perform these tests at the corrosion potential (E_{corr}), 0 mV(SCE), 1000 mV(SCE) and 2000 mV(SCE).

The Nyquist plots obtained at the tested potentials are shown in Fig. 2. At all potentials a near capacitive response was detected, characterized by incomplete semicircles at E_{corr} and 0 mV(SCE), and almost complete semicircles at 1000 mV(SCE) and 2000 mV(SCE).

The Bode plots of EIS measurements are shown in Figs 3 and 4. At least two relaxation time constants are indicated by the two peaks on all phase angle plots (Fig. 3). As the overpotential increases the peaks dislocate into higher frequencies. At potentials of 1000 mV(SCE) and 2000 mV(SCE), the phase angle at low frequencies

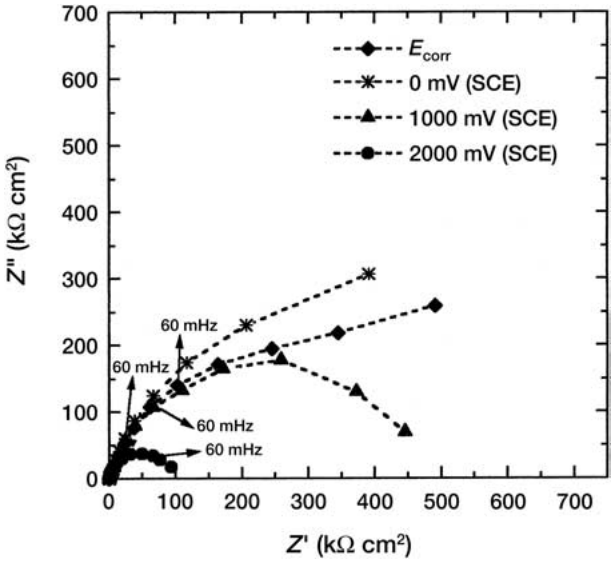

Figure 2 Nyquist plots for Ti–6Al–7Nb alloy tested at different potentials in Hank's aerated solution at pH 7.8 and 25 °C.

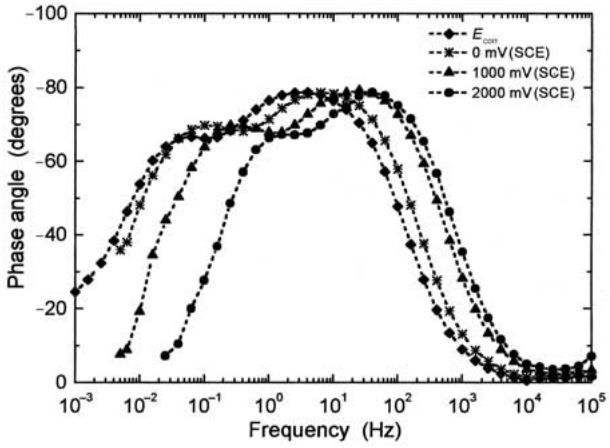

Figure 3 Phase angle Bode spectra for Ti–6Al–7Nb alloy tested at different potentials in Hank's aerated solution at pH 7.8 and 25 °C.

approached 0 degrees. In /Z/ Bode plots (Fig. 4) straight lines are observed with slope approaching -1, in a similar way as for other titanium alloys reported in literature [2, 5].

The obtained spectra were interpreted in terms of an ''equivalent circuit'' with the circuit elements representing electrochemical properties of the alloy and its oxide film. Fig. 5 shows the equivalent circuit used for fitting the spectra obtained at various potentials, which is similar to that proposed by Mansfeld and Kendig [11] for anodized aluminum. R_{bL} and C_{bL} represent the resistance and capacitance of the barrier layer, and R_{pL} and C_{pL}, represent the resistance of the porous layer with the electrolyte inside the pores and the capacitance of the porous layer, respectively. R_s is the resistance of the Hank's solution.

The quality of fitting to the equivalent circuit was judged by the chi-square value. The results of this fitting are presented in Table IV. The obtained values of chi-square indicate a good fitting to the proposed circuit. In Fig. 6, the diagrams of the adjustment results are compared with the experimental data, showing the good quality of this adjustment.

For titanium oxide films, a distributed relaxation feature is commonly observed [1]. Due to this fact, in this study a constant phase element (CPE) was used for data adjustment instead of an ideal capacitor. This approach has also been used by other investigators for

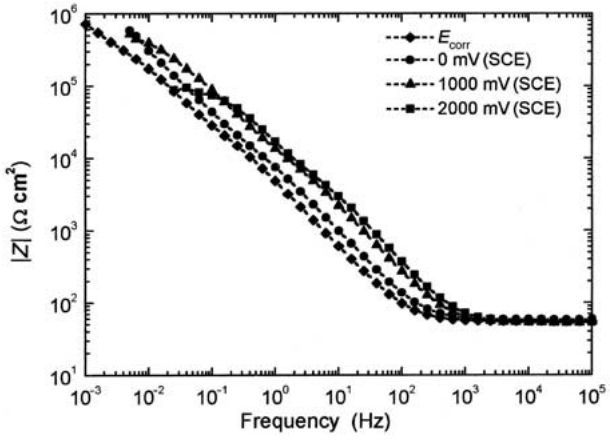

Figure 4 Z Bode spectra for Ti–6Al–7Nb alloy tested at different potentials in Hank's aerated solution at pH 7.8 and 25 °C.

TABLE IV Electrical parameters of equivalent circuit (Figure5) obtained by fitting the experimental results of EIS tests, together with the chi-square values

E mV(SCE)	R_s (Ω.cm^2)	C_{pL} (μF.cm^{-2})	R_{pL} (kΩ.cm^2)	C_{bL} (μF.cm^{-2})	R_{bL} (kΩ.cm^2)	Chi-square
E_{corr}	55	38	57	27	520	0.009
0	58	22	50	16	590	0.020
1000	53	9.5	27	7.8	390	0.010
2000	54	6.1	13	5.7	82	0.019

titanium oxide passive films [1, 2, 12]. The impedance of the CPE is given by $Z_{CPE} = C[(jw)^n]^{-1}$, where C is the capacitance associated to an ideal capacitor, w is the angular frequency and $-1 < n < 1$ [12]. When $n = 1$, CPE is an ideal capacitor. A true capacitive behavior is rarely obtained. The n values close to 1 represent the deviation from the ideal capacitive behavior [2]. Despite of a constant phase element (CPE) being utilized for data fitting instead of an ideal capacitor, since the n values obtained from data fitting were in the range from 0.85 to 0.95, the value obtained from data fitting was taken as the capacitance.

Discussion

The impedance data obtained at various potentials were compared in order to evaluate the influence of the potential on the passive oxide characteristics. The model and equivalent circuit illustrated in Fig. 5 were proposed by Hitzig *et al*. [13] and Mansfeld and Kendig [11] to describe the bi-layer oxide film formed on aluminum. This circuit was also proposed in the literature to represent the oxide film on Ti–6Al–4V [6]. According to the literature [14–16], there is substantial evidence that the film formed on titanium in aqueous solutions, in many exposure conditions, exhibits a two-layer structure composed of a dense inner layer and a porous outer layer. It has been found that the titanium oxide is essentially TiO_2, with a transient region between the inner and the outer layers [4]. This type of oxide was also observed to form on Ti–6Al–7Nb alloy after immersion in NaCl [17] and after anodic polarization [18].

The two-layer model of the oxide film, as shown in Fig. 5, was well supported by EIS results obtained in this investigation. Large values of R_{bL} at potentials around E_{corr} (order of $5 \times 10^5\ \Omega\,cm^2$) were obtained supporting the passivation of the Ti–6Al–7Nb alloy in Hank's solution. R_{bL} was greater than R_{pL} by a factor of nearly 10, showing that the resistance of the oxide film on the Ti–6Al–7Nb alloy is due to this layer. As the potential changed from E_{corr} to 0 mV(SCE), R_{bL} and R_{pL} increased and C_{bL} and C_{pL} decreased. These results seem to correspond to a slight thickening of the titanium oxide film. This is consistent with the fact that in the range from E_{corr} to 0 mV(SCE) the passive current density remains almost constant (Fig. 1). This constant value may be a

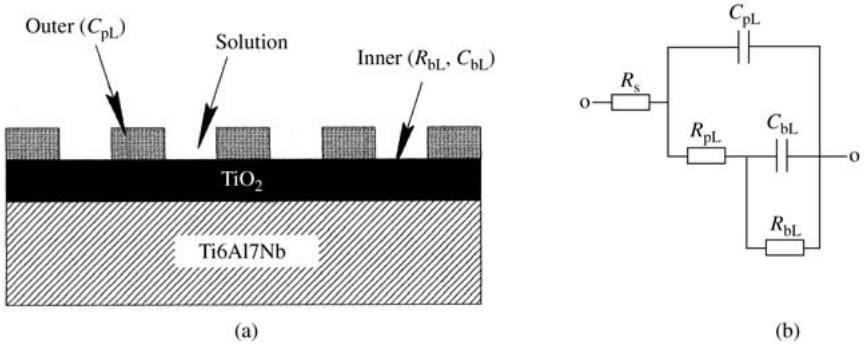

Figure 5 (a) Schematic model of the bi-layer oxide film for Ti–6Al–7Nb alloy in Hank's aerated solution and (b) electrical equivalent circuit.

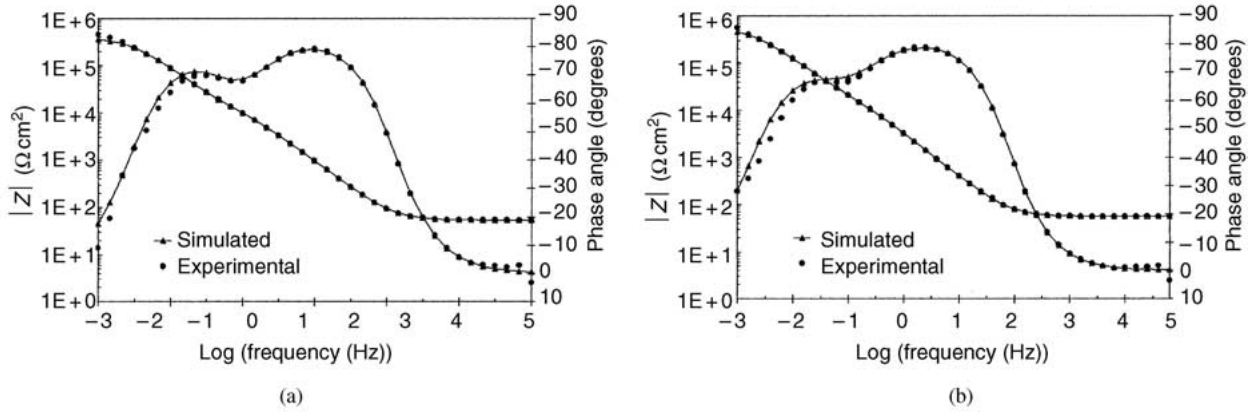

Figure 6 Experimental results and simulated data for Ti–6Al–7Nb alloy tested in Hank's aerated solution at pH 7.8 and 25 °C at different potentials. (a) E_{corr}, (b) 1000 mV (SCE).

consequence of that any increase in the potential is accompanied by progressive thickening of the film, maintaining the electric field within it constant [19]. The values of R_{bL} and R_{pL}, obtained at 1000 mV(SCE) decreased, and that of C_{bL} and C_{pL} increased when compared to those obtained at 0 mV(SCE). The increase in C_{bL} coupled to the decrease in R_{bL} are indicative of barrier layer thinning as the overpotential increased. The polarization curve indicates a current density increase at potentials around 1200 mV(SCE), which could be related to oxide thinning due to chemical breakdown or partial dissolution of the oxide film. The release of titanium ions into the porous layer, due to chemical breakdown of the oxide, could eventually lead to hydration of the barrier layer and to the increase of C_{bL}.

As the potential increases from 1000 mV(SCE) to 2000 mV(SCE), the capacitance and resistance of both layers, barrier and porous, decreases. The decrease in resistance indicates that the oxide layer may become more defective at large overpotentials. The polarization curve shows larger corrosion current densities at 2000 mV(SCE) comparatively to 1000 mV(SCE). Despite of this, a partial recover of the oxide film at potentials over 1800 mV(SCE) is indicated by the polarization curve. This partial recover could be responsible for the decrease in capacitance of both layers, barrier and porous as the potential increased from 1000 mV(SCE) to 2000 mV(SCE).

Despite the decrease of R_{bL} as the applied potential increased, it is still very high at 2000 mV(SCE), of order of $8 \times 10^4\ \Omega\,cm^2$, indicating that the alloy is still highly resistant to corrosion even at very large overpotentials. The high resistance of the barrier layer R_{bL} at all potentials tested implies a high corrosion resistance of the Ti–6Al–7Nb alloy in Hank's solution, i.e. a low rate of titanium release. In fact, Ti ions were not detected in Hank's solution after a six months period of exposure of this alloy [20].

It is worth to note that C_{bL} and C_{pL} have similar values at all potentials tested in this investigation. It is believed that the outer layer (porous) consists of the same oxide as the inner layer (barrier) but with microscopic pores. It is also generally agreed that the pores in the outer layer may be filled with electrolyte, and this might have contributed to the larger values of C_{pL} comparatively to C_{bL}.

While the corrosion resistance of the alloy is ascribed to the barrier layer, its good ability to osseointegrate can be attributed to the presence of the porous layer. It seems reasonable to assume that as soon as the implantation is completed, the bone cells (osteoblast-like cells) tend to migrate inside the pores of the passive film. This interpenetration certainly facilitates the adhesion between the implant and the bone (implant anchorage). In this way, the osseointegration is not only accelerated but also turned more effective, because of an increased and non uniform contact surface.

Although the tests in present work were carried out at 25 °C, it is believed that a similar double layer passive film is also formed at 37 °C (body temperature). This is partially supported by the electrochemical polarization behavior displayed by this alloy in short [10] and long-term [20] tests, which were carried out at 37 °C.

Conclusions

The obtained electrochemical impedance spectroscopy data support the formation on the Ti–6Al–7Nb alloy in Hank's solution of a two-layer oxide film, composed of a dense inner layer and a porous outer layer, similar to that formed on aluminum alloys. The high corrosion resistance, displayed by this alloy in electrochemical polarization tests, is due to the inner layer, while its osseointegration ability can be ascribed to the presence of the outer porous layer.

Acknowledgments

The authors express their gratitude to Fundação de Amparo à Pesquisa do Estado de São Paulo-FAPESP (São Paulo State Foundation for Support of Research). The Research Grant FAPESP 99/08554-6 supported this study. One of the authors (Lavos-Valereto) acknowledges the postdoctoral grant FAPESP 99/03771-9.

References

1. J. PAN, D. THIERRY and C. LEYGRAF, *Electrochim. Acta* **41** (1996) 1143.
2. J. E. G. GONZÁLEZ and J. C. MIRZA-ROSCA, *J. Electroanal. Chem.* **471** (1999) 109.
3. I. C. LAVOS-VALERETO, B. KÖNIG JR, C. ROSSA JR, E. MARCANTONIO JR and A. C. ZAVAGLIA, *J. Mater. Sci. Mater. Med.* **12** (2001) 273.
4. J. PAN, D. THIERRY and C. LEYGRAF, *J. Biomed. Mater. Res.* **28** (1994) 113.
5. T. M. SILVA, J. E. RITO, A. M. P. SIMÕES, M. G. S. FERREIRA, M. DA CUNHA BELO and K. G. WATKINS, *Electrochim. Acta* **43** (1998) 203.
6. R. VENUGOPALAN, J. J. WEIMER, M. A. GEORGE and L. C. LUCAS, *Biomaterials* **21** (2000) 1669.
7. M. SEMLITSCH, F. STAUB and H. WEBER, 5th European Conference on *Biomaterials*, Paris (Sept. 1985) p. 69.
8. K. WAGNER, *Clin. Orthop.* **271** (1991) 12.
9. Z. CAI, T. SHAFER, I. WATANABE, M. E. NUNN and T. OKABE, *Biomaterials* **24** (2003) 213.
10. I. C. LAVOS-VALERETO, I. COSTA and S. WOLYNEC, *J. Biomed. Mater. Res. (Appl. Biomater.)* **63** (2002) 664.
11. F. MANSFELD and M. W. KENDIG, *J. Electrochem. Soc.* **135** (1988) 828.
12. J. GLUSZEK, J. MASALSKI, P. FURMAN and K. NITSCH, *Biomaterials* **18** (1997) 789.
13. K. HITZIG, W. J. JUTTNER, W. LORENZ and J. PAATSCH, *J. Electrochem. Soc.* **133** (1986) 887.
14. N. D. TOMASHOV, G. P. CHERNOVA, Y. S. RUSCOL and G. A. AYUYAN, *Electrochim. Acta* **19** (1974) 159.
15. M. M. HEFNY, A. A. MAZHAR and M. S. EL-BASIOUNY, *Br. Corros. J.* **17** (1982) 38.
16. M. S. EL-BASIOUNY and A. A. MAZHAR, *Corrosion* **38** (1982) 237.
17. P. MAEUSLI, P. BLOCH, V. GERET and S. STEINEMANN, *Adv. Biomater.* **6** (1986) 57.
18. C. KUPHASUK, Y. OSHIDA, C. J. ANDRES, S. HOVIJITRA, M. BARCO and D. BROWN, *J. Prosthet. Dent.* **85** (2001) 195.
19. J. M. WEST, ''Electrodeposition and corrosion processes'', 2nd edn. (Van Nostrand, London, 1970) p. 87.
20. I. C. LAVOS-VALERETO, C. K. TERUI, I. COSTA and S. WOLYNEC, Long-term performance of Ti–6Al–7Nb alloy implants with and without hydroxyapatite coating in Hank's solution (submitted).

Received 12 September 2002
and accepted 9 July 2003